Computer Standards & Interfaces 000 (2017) 1–8

Contents lists available at ScienceDirect

Computer Standards & Interfaces

journal homepage: www.elsevier.com/locate/csi

A new control mark for photogrammetry and its localization from single image using computer vision

Rostislav Dandoš*, Karel Mozdřeň, Hana Staňková

VŠB – Technical University of Ostrava, Ostrava, Czech Republic

ARTICLE INFO

Keywords:
Control mark
Camera
Computer vision
Detection
Measurement

ABSTRACT

Computer Vision takes part in many industrial applications mainly in robotics and measurement systems. Geodesy uses computer vision rather indirectly using specialized software tools for measurements of data captured with digital cameras or LIDAR systems. This paper describes new control mark and its advantages for deformation measurements, and surface reconstruction. Furthermore, we describe control mark detection method using computer vision algorithms, and its localization from single image. We also compare this method to spatial polar method.

1. Introduction

Reconstruction of surface and structure of objects is important task in many industrial applications. Very popular method for surface or object reconstruction is known as photogrammetry well described in Kapica and Sladkova [5]. The information we obtain from most photogrammetric systems using control marks are three-dimensional positions of the marks. We have focused on stereo-metrical system with control marks, where the main measurement tool is a camera. The user takes multiple images of the measured object with control marks from different angles, and then the three-dimensional coordinates of each mark are computed. This measurements are done repeatedly over time to measure the shift and deformation of the monitored object well described in DIAS-DACOSTA [14]. The important part of every photogrammetric system is detection of control marks using computer vision techniques. Good detection rate and precise measurement of the control mark are essential for reliable results. We have been working on an improvement of detection rates of control marks and a way for extraction of more data from them.

Every control mark have to be easily distinguishable from the environment it is located in. Therefore, the control mark is often realized as an image with high contrast colors or intensities (in most cases black and white), MORIYAMA [15]. Also, the shape of the mark should be very different from shapes of the objects that are naturally present in surveyed locations. These premises allows photogrammetric tools to easily detect those marks in the image with higher reliability (lower number of false detections). Hereby we can say that the use of control marks with simple shape like circle is highly unreliable and the user is forced to mark the marks on the image manually.

We have designed a new control mask, which is more complex, and therefore, it is less likely that there will be similar objects in the image causing false detection. Furthermore, the mark is designed in such a way, that we can easily extract its three-dimensional rotation. This is useful mainly when we are measuring deformation of the object of interest. We also propose a photogrammetric method using only single camera image for three-dimensional localization. We describe the new control mark, and new localization method in greater detail in following sections.

Testing detection of newly proposed targets took place both in the laboratory conditions and outdoors on the retaining wall no. 8246 in the undermined part of the D1 motorway in Ostrava, the city district of Svinov. The results of the testing show that the location of targets and their detection can also be successfully applied to more complex constructions in the real environment.

2. Control mark

The control mark must be easily visible and distinguishable from the environment we are going to place it into. Therefore, the mark must have high contrast colors or intensities and its shape should be more complex than objects usually present in most locations to make it more distinguishable from the surveyed environment. It must provide more than one coordinate, so it would be possible to extract its rotation in three-dimensional space, and to estimate it position from single image, for difficult situations, when it is not possible to take more images from different angles (e.g. narrow areas).

* Corresponding author.
E-mail addresses: rostislav.dandos@vsb.cz (R. Dandoš), mozdren@gmail.com (K. Mozdřeň), hana.stankova@vsb.cz (H. Staňková).

http://dx.doi.org/10.1016/j.csi.2017.09.003
Received 27 February 2017; Received in revised form 6 September 2017; Accepted 6 September 2017
Available online xxx
0920-5489/

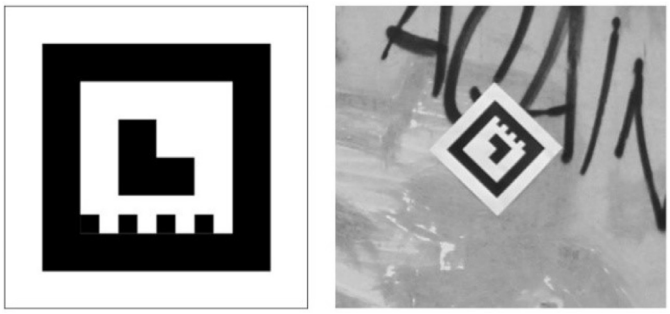

Fig. 1. Proposed control mark and its placement on the testing wall.

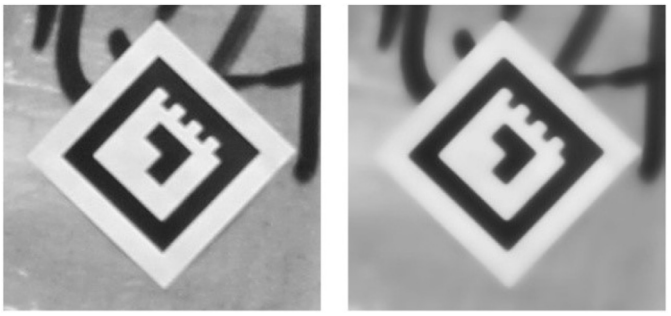

Fig. 3. Control mark before and after filtering.

We have designed a control mark, which meets all given requirements. As seen in Fig. 1, it is rectangular with specially designed internal pattern to ensure its uniqueness. It is also diagonally asymmetrical, and therefore, we can conclusively extract its rotation. Consequently, each point on the mark can be uniquely identified. The border around the mark ensures its relatively easy distinction from other objects in the image. We describe the detection algorithm in the following section.

3. Control mark detection

The object detection is important task in computer vision. There are numerous methods for this task. Well researched domains of object detection include face detection described in Yang et al. [12] and pedestrian detection described in Enzweiler and Gavrila [3]. The most known detector tools are SVM developed by Cortes and Vapnik [2] and AdaBoost developed by Viola and Jones [11]. These detectors are trained, and therefore, they need training sets consisting of positive samples (consisting the object of interest) and negative samples (other objects or parts of background image) to work. There are also moving object detectors based on background subtraction described in Malik et al. [6]. These methods are learning the background of the image (slowly moving or stationary objects) and subtracts the foreground (moving objects). Another, method for object detection is to analyze a contour of the object extracted from image segmentation or directly from image gradient. The last mentioned method is most suitable for our task, because it is working correctly also for rotated and scaled images. This is important, because our marks can be positioned from different distances, angles, and with different rotations as it can be seen in Fig. 2.

Our detection method consists of few fundamental steps. First, we filter the image noise to reduce its influence on detection. Then we extract important edges and corners from the image. After that, we find continuous contours from edges consisting only four corners (rectangular control mark). Extracted contours are candidates for our detected mark. The last step is to test each candidate against predefined pattern (expected appearance of the control mark) using algorithm known as pattern matching. This step is done for multiple permutations of the corner points to find the right orientation of the control mark. This method is described in further detail in following subsections.

3.1. Image filtering

Image filtering is a process used for reduction of undesirable properties of the image. Image noise is random component of the image causing variation of color and brightness. It is error caused by sensor chip of the camera. If this noise is not filtered out, the edge and corner detectors will not work properly. Therefore, we use image filtering to reduce noise.

The most used image filter for noise reduction is Gaussian filter described in Stockman and Shapiro [10]. The Gaussian function is used as a kernel function for image convolution with noisy image. Gaussian filter reduces random image noise very effectively, but with the noise also the edges in the image are blurred. This is due to properties of edges and noise in frequency domain of the image. Both noise and edges are represented by frequencies and the Gaussian blurring works as a low-pass filter in frequency domain. To preserve edges in the image other method for filtering must be used.

The filter we have used is known as Perona-Malik filter developed by Perona and Malik [8]. This filter preserves important details in the image, typically edges and lines, which is important for our method. This filter is based on heterogeneous diffusion described by following equation

$$\frac{\partial I}{\partial t} = \nabla \cdot (c \nabla I), \tag{1}$$

where I represents image, t is time, ∇ represents gradient operator, and c is diffusion coefficient. The diffusion coefficient is very important in the equation. It describes behavior along the edges in the image. The basic idea is to slow down the diffusion process (filtering) along the edges. This way, similar intensities are filtered more, and therefore, creating homogeneous areas separated by preserved significant edges. The diffusion coefficient is driven by image gradient magnitude and has the following form

$$c(\| \nabla I \|) = \frac{1}{1 + \left(\frac{\| \nabla I \|}{K} \right)^2}, \tag{2}$$

where K represents a sensitivity to edges. The result of image filtering using the Perona-Malik filter can be seen in Fig. 3. As you can see, the detail of control mark is much more homogeneous than in original image, yet the edges are preserved. This step significantly improves edge and corner detection.

3.2. Edges and corners detection

Corners and edges are important features for our control mark detector. Edges are parts of the image, where image intensities change rapidly (high gradient magnitude). We are often looking for thin edges

Fig. 2. Views on control marks from different angles.

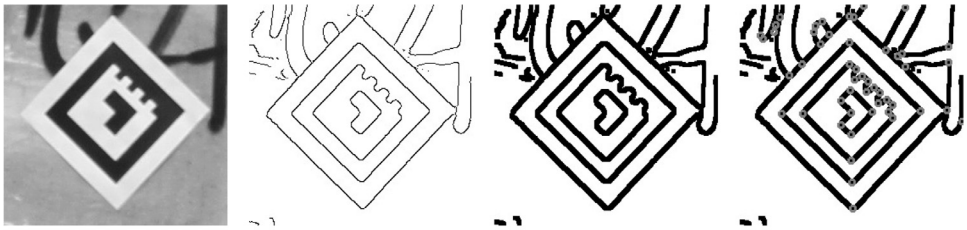

(a) (b) (c) (d)

Fig. 4. Edges and corners detection: (a) Original image; (b) Canny edge detector output; (c) Canny edge detector output dilated; (d) Harris corner detection output.

corresponding with boundaries of the objects in the image. On the other hand, corners are areas in the image, where the edges rapidly change its shape, for example intersection of two lines. Combination of edges and corners is essential for control mark detection. The basic idea is to find continuous contour having exactly four corners, because it is exact representation of our control mark boundaries.

We have used Canny edge detector developed by Canny [1] also known as optimal detector, because it is adaptable to various environments. This algorithm consists of four basic steps. The First step is to filter the image. The authors proposed to use Gaussian filter, but we have already filtered the image using the Perona-Malik filter. The second step is to find image gradient magnitudes and orientations. The Sobel operators are used for this task. Convolution of Sobel operators with the input image creates two output images with approximated partial derivations D_x for x-axis and D_y for y-axis. This step can be described by following equations

$$D_x = I * \begin{pmatrix} -1 & 0 & 1 \\ -2 & 0 & 2 \\ -1 & 0 & 1 \end{pmatrix}, D_y = I * \begin{pmatrix} -1 & -2 & -1 \\ 0 & 0 & 0 \\ 1 & 2 & 1 \end{pmatrix}, \tag{3}$$

where I is the input image, and $*$ is a convolution operator. To compute approximate magnitude and orientation of the gradient the following formulas are used

$$G(x, y) = \sqrt{D_x(x, y)^2 + D_y(x, y)^2}, \tag{4}$$

$$\Theta(x, y) = \arctan\left(\frac{D_y(x, y)}{D_x(x, y)}\right) \tag{5}$$

where G is gradient magnitude image, and Θ is gradient orientations image. The orientations are often rounded to one of four angles (0, 45, 90 or 135). Third step is to apply Non-maximum suppression to filter out every pixel that is not in local gradient maximum. Only pixels which form thin edges remain. The last step is to threshold pixels according to gradient magnitudes. There are two thresholds: upper and lower. If a pixel gradient is above the higher threshold, then the pixel is accepted as edge. If a pixel gradient is under the lower threshold, it is rejected. If it is between lower and upper threshold, it is accepted only if the pixel is connected to pixel with gradient above upper threshold. The result of Canny edge detector can be seen in Fig. 4b. We must make the edges more thick, because we are going to use the edges in combination with corners, and they must be on the border of the control mark. We have used dilatation for this task. The result of dilatation can be seen in Fig. 4c.

The corner can be defined as a point in the image, where two edges intersect, or as a point in the image which has at least two significant edges in the neighborhood with different orientations. The algorithm we have used is called Harris corner detector or it is also referred to as Harris operator developed by Harris and Stephens [4]. This operator is improved Moravec corner detector proposed by Moravec [7]. This improved corner detector uses differentials of the corner score with respect to direction. First step is to compute approximation of a sum of squared differences (SSD), denoted as S, which is computed as form

$$S(x, y) \approx \sum_u \sum_v w(u, v)\big(D_x(u, v)x + D_y(u, v)y\big)^2, \tag{6}$$

where w is a window function (usually Gaussian), D_x and D_y are images of partial derivatives of input image, and x and y are image coordinates. This can be easily rewritten into matrix formula

$$S(x, y) \approx (x \quad y)A(x \quad y)^T, \tag{7}$$

$$A = \sum_u \sum_v w(u, v)\begin{pmatrix} D_x^2 & D_xD_y \\ D_xD_y & D_y^2 \end{pmatrix}. \tag{8}$$

Typically, the corner is indicated, when the S has high variations in all directions of the vector $(x\ y)$. Following step is to analyze eigenvalues of the matrix A. If both eigenvalues λ_1 and λ_2 have values near 0, then the point has no feature of interest. If λ_1 is near to 0 and λ_2 has large positive value, then the point is marked as edge. Finally, if both λ_1 and λ_2 have large positive number, the point is marked as corner. It is suggested that we should not compute eigenvalues exactly, and use following computation instead and analyze its value

$$M_C = \det(A) - \kappa Trace^2(A), \tag{9}$$

where M_c is the value we have to analyze, and κ is sensitivity coefficient, which should be set between $0.04 \sim 0.15$ as the authors suggest. The result of corner detector combined with edge detector can be seen in Fig. 4d.

3.3. Detection

As an input for detection the edges and corners with input image are used. The detection itself can be described in three basic steps. First, we find all contours with four corners, then we find corresponding permutation for the corner points to match the contour orientation with template orientation, and finally, we compare the template pattern with detected object within the detected contour.

First we find the contours using connected components algorithm. Subsequently, we compute the number of corner in each contour, and if it is four, we mark the object as a candidate for the control mark. An example of result from this step can be seen in Fig. 5. In our example, the number of candidates is reduced to one.

Now we only have the objects with four corners, and we must find only those, that look the same as our control mark. We use pattern matching for this task. The problem is, that we do not know the order of corners of the object, and also, the object in the image is transformed (rotated, scaled). These problems must be dealt with. We use a combination of corner permutations and perspective transformation known as homography.

Homography is a transformation for projection between two planes. It is often used in road surface monitoring systems, where we want to have a *bird-like* (up-down) view on the road around the car. To find a perspective transformation we need at least four points in the input image and four points in the output image for exact computation of the homography matrix H. The matrix H represents a transformation matrix

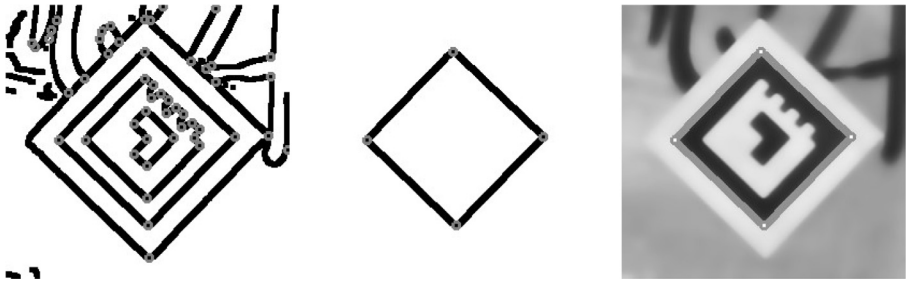

Fig. 5. Extracted candidate contour for control mark detection, and its visualization onto the mark in the image.

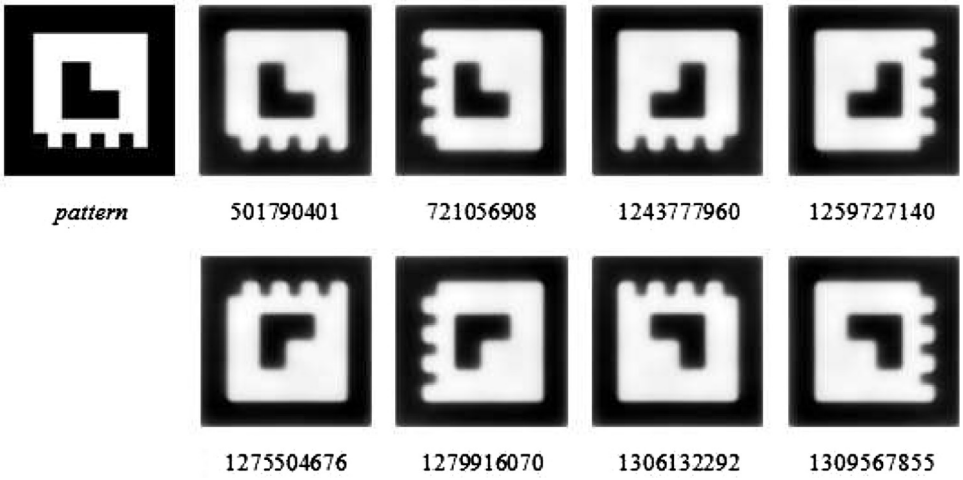

Fig. 6. Transformed images and theirs corresponding SSD in comparison with used template pattern in ascending order.

for the points from one image plane to the other in such a way, that the transformation transforms the input points onto the output points with minimal projection error. The homography can be described using following formulas

$$p_a = \begin{pmatrix} x_a & y_a & 1 \end{pmatrix}^T, \tag{10}$$

$$p'_b = \begin{pmatrix} w'x_b & w'y_b & w' \end{pmatrix}^T, \tag{11}$$

$$H_{ab} = \begin{pmatrix} h_{11} & h_{12} & h_{13} \\ h_{21} & h_{22} & h_{23} \\ h_{31} & h_{32} & h_{33} \end{pmatrix}, \tag{12}$$

$$p'_b = H_{ab}p_a, \; where \; H_{ab} = H_{ab}^{-1}, \tag{13}$$

$$p'_b = \frac{p'_b}{w'}, \tag{14}$$

where p_a is input point from input image plane, p'_b is output point in output image plane, H_{ab} is projective transformation used for transformation of the point p_a onto the point p'_b, x and y are image coordinates, and w' homogeneity coefficient for conversion of point p'_b to point p_b. To find the homography matrix H the basic Direct Linear Transformation Algorithm (DLTA) is used.

The idea of distinction between control marks and other objects is given by comparison of sample pattern with data extracted from the image (pattern matching). First we must transform object defined by detected contour from input image into the same image space as the sample pattern (register both images using homography). Since both images are registered we can compare them pixel by pixel using the previously mentioned SSD. This comparison is done for each possible and logical permutation of the corners (no edge is crossing the other edge), and as the result, the order of the corners with the lowest SSD is used. Furthermore, the lowest SSD is also used for decision if the detected object is our control mark (thresholding is used). The transformed images in comparison with template image with measured SSD can be seen in Fig. 6. In this figure, the transformed image nearest to control mark pattern (the one with least SSD) is the one we consider to have corners in the correct order. Now we know positions of the point on the control mark in the image, therefore, we can use it to measure the location of the mark itself (e.g. using stereoscopy).

4. Measuring control mark position from single image

We need to know positions of control marks to reconstruct three-dimensional model of measured object, and also to measure its occasional deformation. In many cases, it is difficult to measure in hardly accessible places with limited room for camera manipulation. Therefore, we were highly motivated to develop a simple method for control mark localization using only single camera image.

As we have mentioned earlier, the increased complexity of control mark makes it more difficult for detection, but on the other hand, more complex control mark decreases the probability there will be any other object in the image causing false detection. Another asset with complex marks is that we know its structure and also distances between its corners (points of interest). Knowing enough information about the object we are trying to detect and about camera we are using for measurement allows us to measure its position.

The first part of the information we have to acquire the intrinsic and extrinsic camera parameters. We would need these two also if we were using stereoscopy for measurement. These parameters are important for distortion compensation and also for information about focal length and center of the view-port. These data are essential for reconstruction of the measured object. Without these data the measurement would be unnecessarily inaccurate. Number of points of interest is also very important

part in object localization. We need at least four point and theirs relative positions to find three-dimensional position of an object.

In our case, we have four points in each detected object and also all camera parameters. This is enough to find three-dimensional position of the control mark. We use re-projection for the localization itself. The idea is to project the known shape of the control mark (corner points) onto the view-port in such a way, that it matches the detected mark in the image. Therefore, we need to find unknown projection parameters, namely, translation and rotation vector. Parameters for camera matrix are known from camera calibration. Many optimization method can be used to find the unknown translation and rotation vectors. We have used genetic algorithm described in Schmitt [9], which is heuristic search method inspired in natural selection. Every evolutionary algorithm uses some kind of fitness function to evaluate the fitness (quality) of the solution. We will discuss these ideas in greater detail in following subsections.

4.1. Genetic algorithm

Genetic algorithm is a method for heuristic search for optimal results. The method works with multiple results at the same time. Each result is encoded in structure known as chromosome and all results together form a new generation (population). Each generation has one or more representatives from previous generation known as parents, which represent the former best results. Each new generation is created using the parents (best results) from former generation. To fulfill this task, the crossover, mutation, and selection operators are used.

Crossover operator also known as recombination represents the combination of the best results (parents) to create new generation (results). According to encoding if the information the crossover operator varies. For example, if the information is encoded in binary manner (each bit represents gene), then the crossover operator will randomly select each bit from one of the parents and copies it to a new chromosome in the upcoming generation. Whole new generation is created this way.

Another important operator is mutation. This operator introduces diversity into the population. The diversity is important for heuristic search. After crossover each of the chromosomes are combination of the best chromosomes, but these chromosomes without mutation are all the same, and therefore, the mutation is introduced. This operator changes each chromosome (result) a bit so each population covers greater part of search space. In the case of binary encoding, random bits (genes) are inverted. This prepares the ground for the final operator, the selection.

Selection operator selects new parents for the next generation. In nature only the best individuals survive. The same principle applies for genetic algorithms. Only the best chromosomes are selected to be used in next generation. We need some kind of a measure to evaluate the fitness of each individual. This measure is a fitness function, which is different for each application. For example, for the problem of finding a maximum of a function the fitness function is the evaluation of the function itself. The higher is the value the higher is the fitness. We will discuss our application of genetic algorithm in the following subsection.

4.2. Estimation of projective matrix

The camera parameters as focal length and center of the view-plane are already known, but we have to estimate rotation and translation vectors. Estimation of these parameters will allow us to find location of object of interest. The first step is to put control mark model into the center of projection and then estimate the translation and rotation which will put projected model onto detected object in the image. We find these parameters using genetic algorithm.

First problem we have to solve is the encoding. We have six parameters in total: rotation along three axes ($\alpha\ \beta\ \gamma$), and translation vector ($t_x\ t_y\ t_z$). We encode these parameters as an array of float values. So each chromosome in population has six genes represented as float values. The mutation operator is then defined as an addition of random vector to chromosome. And for the selection operator (fitness function) the re-projection error is used. *Re*-projection error uses points in defined space Ω and points in different space Γ projected to space Ω using transformation matrix P (projection) P: $\Gamma \rightarrow \Omega$. The squared differences between actual and projected points are then used for fitness function. This re-projection error can be expressed using following equation

$$E_R = \sum_{i=1}^{N} \left| x_i - P(x'_i) \right|^2, \tag{15}$$

where $x_i \in \Omega$ is an image point detected on control mark, $x_i^0 \in \Gamma$ is control mark point in three-dimensional space, which can be transformed onto the view-port (two-dimensional image) using transformation matrix P. Finally, N represents number of control points present on the control mark, which is four in our case. Hereby, we can say, that we are looking for such transformation P_{min} with minimal re-projection error, for which the following equation is valid

$$P_{\min} = \arg\min_{P} \sum_{i=1}^{N} \left| x_i - P(x'_i) \right|^2, \tag{16}$$

where *argmin* represents the search of the transformation matrix P_{min} in search space Γ containing all possible transformations. In our case, this function is realized using genetic algorithm. As soon as we find the transformation, we can find three-dimensional position of control mark with transformation of control mark using only rotation and translation.

5. Experiments

The accuracy of detection of new control marks and determination of their spatial position were conducted under laboratory conditions. To verify the accuracy of the values obtained from detection the geodetic method known as spatial polar method was used. The test included brackets for control marks and simple micro-network for geodetic measurements. Brackets allow any shifts and rotations of control marks. Micro-network consists of two reflective plates representing the approximate line. Diagram of the test unit is shown in Fig. 7.

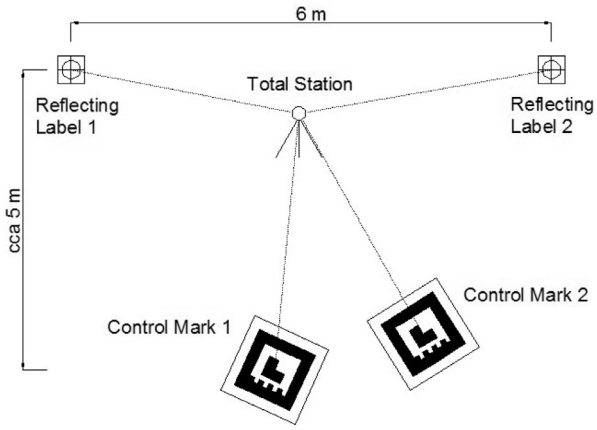

Fig. 7. Scheme of laboratory testing environment.

5.1. Spatial polar method

The spatial polar method shown in Fig. 8 is based on the measuring of slope length d from the known point (survey station S), horizontal angle (for the determination of the bearing) and zenith angle z to the determined point (detailed survey point P). The equations for the calculation of coordinate differences between the survey station S and the determined point P resulting from proposed scheme are as follows

$$\Delta X_{SP} = d_{SP} \cdot \sin(z) \cdot \cos(\sigma_{SP}), \tag{17}$$

Table 1
First attempt of methods comparison.

Frame number	*Spatial distance between control mark centers* [m]		ε [m]	$\varepsilon\varepsilon$ [m^2]
	Fotogrammetically	*Geodetically*		
1	$351.4{\cdot}10^{-3}$	$338.0{\cdot}10^{-3}$	$-13.4{\cdot}10^{-3}$	$179.56{\cdot}10^{-6}$
2	$339.6{\cdot}10^{-3}$	$338.0{\cdot}10^{-3}$	$-1.6{\cdot}10^{-3}$	$2.56{\cdot}10^{-6}$
3	$338.6{\cdot}10^{-3}$	$338.0{\cdot}10^{-3}$	$-0.6{\cdot}10^{-3}$	$0.36{\cdot}10^{-6}$
4	$344.0{\cdot}10^{-3}$	$338.0{\cdot}10^{-3}$	$-6.0{\cdot}10^{-3}$	$36{\cdot}10^{-6}$
			$\Sigma\varepsilon\varepsilon=$	$221.48{\cdot}10^{-6}$

Table 2
Second attempt of methods comparison.

Frame number	*Spatial distance between control mark centers [m]*		ε [m]	$\varepsilon\varepsilon$ [m^2]
	Fotogrammetically	*Geodetically*		
1	$379.5{\cdot}10^{-3}$	$372.0{\cdot}10^{-3}$	$-7.5{\cdot}10^{-3}$	$56.25{\cdot}10^{-6}$
2	$377.1{\cdot}10^{-3}$	$372.0{\cdot}10^{-3}$	$-5.1{\cdot}10^{-3}$	$26.01{\cdot}10^{-6}$
3	$379.7{\cdot}10^{-3}$	$372.0{\cdot}10^{-3}$	$-7.7{\cdot}10^{-3}$	$59.29{\cdot}10^{-6}$
4	$377.9{\cdot}10^{-3}$	$372.0{\cdot}10^{-3}$	$-5.9{\cdot}10^{-3}$	$34.81{\cdot}10^{-6}$
			$\Sigma\varepsilon\varepsilon=$	$176.36{\cdot}10^{-6}$

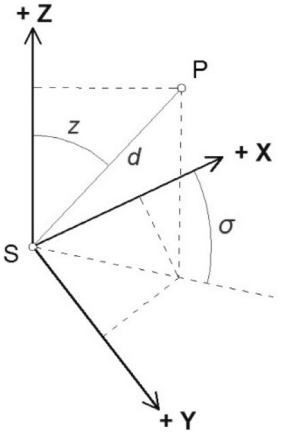

Fig. 8. The scheme of spatial polar method.

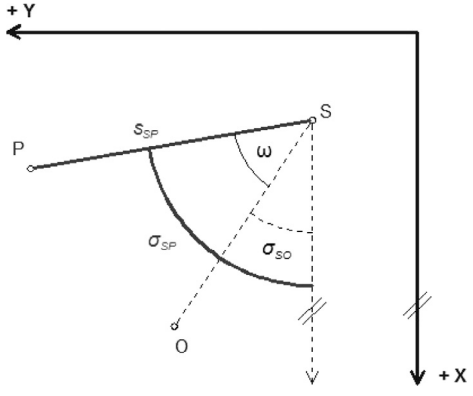

Fig. 9. The principle of bearing calculation.

$$\Delta Y_{SP} = d_{SP} \cdot \sin(z) \cdot \sin(\sigma_{SP}), \tag{18}$$

$$\Delta Z_{SP} = d_{SP} \cdot \cos(z), \tag{19}$$

The bearing σ, as shown in Fig. 9, is an angle which is closed by the parallel with the positive semi-axis X pointing to the south, passing through the station S, and by the requested side. The bearing therefore cannot be directly measured, hence the horizontal angle ω from another known point (orientation O) is observed. The bearing σ_{SP} is calculated from the bearing σ_{SO} (determined from the known coordinates of the points S and O) and the measured horizontal angle ω using the expression

$$\sigma_{SP} = \sigma_{SO} + \omega, \tag{20}$$

Basic equations for space coordinates computation of a detailed (measured) survey point have the form

$$X_P = X_S + \Delta X_{SP}, \tag{21}$$

$$Y_P = Y_S + \Delta Y_{SP}, \tag{22}$$

$$Z_P = Z_S + \Delta Z_{SP}, \tag{23}$$

Using substitution we can rewrite these equations into the following form

$$X_P = X_S + d_{SP} \cdot \sin(z) \cdot \cos(\sigma_{SP}), \tag{24}$$

$$Y_P = Y_S + d_{SP} \cdot \sin(z) \cdot \sin(\sigma_{SP}), \tag{25}$$

$$Z_P = Z_S + d_{SP} \cdot \cos(z) + v_p, \tag{26}$$

In the equation for the Z-coordinate, the height of the instrument v_P above the stabilization mark defining the survey station must be added to the basic term.

5.2. Measurements

Coordinates of the center marks measured using geodetic method were calculated in *Groma 9.1* software. Furthermore, the calculated coordinates of the spatial distance between the two marks were compared with the length computed from coordinates of control marks detected by our photogrammetric method. Table 1 contains first attempt for a comparison of both methods on a series of 4 images. From the measured data we can compute the mean error as follows

$$m = \pm\sqrt{\frac{1}{n}\sum_{i=1}^{n}\varepsilon_i\varepsilon_i} = \pm\sqrt{\frac{1}{4}221.48} = \pm 7.4 \cdot 10^{-3} m. \tag{27}$$

In our second attempt the position of control marks were changed and the results of this measurements are shown in Table 2. In this case, the mean error m is $6{\cdot}10^{-3}$ m.

These are measurements in laboratory conditions. The camera's distance from targets was about 5 m. Only the ability to detect new targets was tested in the real situations.

Fig. 10. Detection of targets on the retaining wall no. 8246.

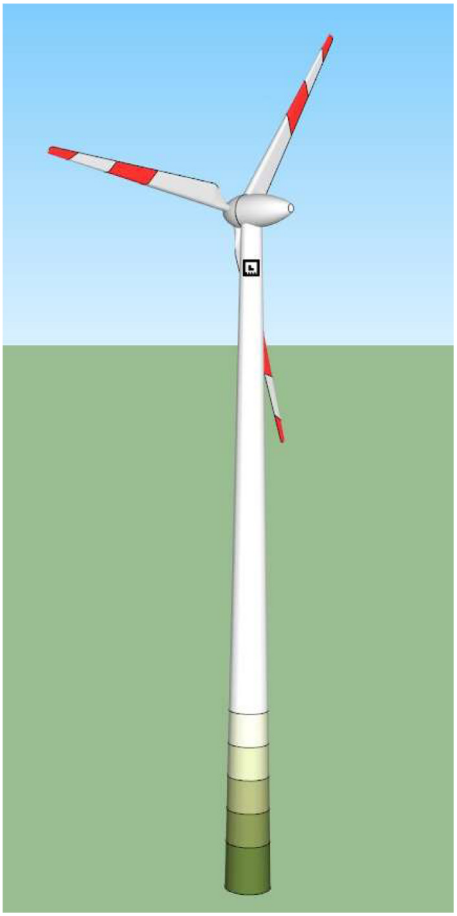

Fig. 11. Sample location of the target.

We can deduct from our measurements that the accuracy of our method is about $\pm 7 \cdot 10^{-3}$ m. The mean error was achieved when scanning from a relatively short distance under laboratory conditions. In the future, we are planning modifications to our software which are going to improve accuracy. Recently, we have prepared a new test platform that allows us to measure control markers in laboratory conditions for longer distances. Then the method will be tested in a similar manner also in the exterior and compared with geodetic methods.

6. Testing

Detecting the image, or a suitable target in space can also be used for example for monitoring the structural deformation. The spatial shifts of structures occurs mainly due to anthropogenic and natural factors. In the Upper Silesian Coal Basin, it is mainly the case of the effects of mining activities. Although most of the coal mines in the Ostrava-Karvina district are already closed, according to Schenk [13], it can take several years before the impact of mining in the subsidence trough fades away.

Monitoring shifts, not only on the undermined territory, can prevent deformation and, in extreme cases, the devastation of the structure. A number of methods, either geodetic or physical, are used for the measurement of the values used for the calculation of the shifts.

For further testing of the detection of new targets, the retaining wall no. 8246 on the D1 motorway in Ostrava was used, which is part of the flyover in Rudná. The retaining wall is located in close proximity to the safeguard pillar of the former Oderský Pit and Svinov Pit. Both pits were already liquidated in 1992, so it is assumed that the effects of mining on the surface have faded away. The retaining wall no. 8246, however, is a very important part of the viaducts and one of the reasons for monitoring the shifts is its position in the undermined area. Monitoring spatial displacements takes place at 56 points since 2004.

The monitored points, which are stabilized by reflective labels, have been supplemented by new code targets with dimensions of 0.15 m × 0.15 m. They were also photographed using the digital camera Canon EOS 7D. Photographing had to be done in stages because of the size of the wall.

The detection of the bull's-eyes, as shown in Fig. 10, was carried out without problems even on such a large object, and their position in space was determined for all of them. Their position was also determined using the spatial polar method by the total station Leica TS 30 (angle accuracy: 0,15 mgon; distance accuracy: 1 mm + 1 ppm), and the mean error of the detection of targets was determined. The mean error of new

photogrammetric methods for testing on the retaining wall no. 8246 was ± 0.007 m.

However, the problem arose when calculating the shifts. It is not yet possible to define reference points or the coordinate system in the software. For the calculation of shifts in the coordinate system of the darkroom, the targets would have to be photographed at various stages in the same position of the darkroom.

Since the first trials, however, the software has been adjusted for the detection of the mark. The software innovation should lead to better and more accurate results. It will include the possibility of defining the reference points, coordinate system and scale.

Currently, a new test base is being prepared, which allows photographing marks in laboratory conditions and for longer distances. Then the method will be tested in a similar way also in the exterior and compared with geodetic methods.

6.1. The method application

The newly proposed one-snap photogrammetric method can have a wide range of applications. The fundamental difference from terrestrial intersection photogrammetric method is to determine the spatial coordinates of the center of the target from only one image. Newly developed software also determines the spatial coordinates in addition to also rotate targets in space. The new method can thus be used for monitoring the displacement of various types of structures. However, targets of a suitable material would have to be placed on the object. A sample location of the target is shown in Fig. 11.

Aesthetically, it would be possible to adapt the color of the target not to disturb the overall impression of the structure. However, their basic shape must be respected. The big advantage of the newly proposed method is the possibility of continuous monitoring of the targets. In the next phase of testing, this possibility will be tested with a CMOS sensor, or a simple darkroom. In the case of quality results, there is the possibility of connecting the darkroom with the GSM module that would send the images to the server with the evaluation software.

7. Conclusions

We have developed a new photogrammetric method for localization of control marks from single image. We have also designed a new control mark that can be used with our new method. The newly designed control mark allows us to measure not only its position, but also to measure its rotation, which can be very useful for measured surface reconstruction. The ability to measure the position of control marks from single image allows to measure tide or generally small areas, where more images from more different angles cannot be taken. We have compared our method to spatial polar method and we deduced that the accuracy of our method is about $\pm 7 \cdot 10^{-3}$ m.

References

[1] J. Canny, A. computational approach to edge detection, Pattern Anal. Mach. Intell. IEEE Trans. PAMI 8 (1986) 679–698.
[2] C. Cortes, V. Vapnik, Support-vector networks, Mach. Learn. 20 (1995) 273–297.
[3] M. Enzweiler, D. Gavrila, Monocular pedestrian detection: survey and experiments, Pattern Anal. Mach. Intell. IEEE Trans. PAMI 31 (2009) 2179–2195.
[4] C. Harris, M. Stephens, A combined corner and edge detector, in: In Proc. of Fourth Alvey Vision Conference, 1988, pp. 147–151.
[5] R. Kapica, D. Sladkova, Photogrammetric analysis of objects in undermined territories, Geodesy Cartography 37 (2011) 49–55.
[6] A.A. Malik, A. Khalil, H.U. Khan, Object detection and tracking using background subtraction and connected component labeling, Int. J. Comput. Appl. 75 (2013) 1–5 Published by Foundation of Computer Science, New York, USA.
[7] H.P. Moravec, Obstacle Avoidance and Navigation in the Real World by a Seeing Robot Rover Ph.D. thesis. Stanford, CA, USA. AAI8024717, 1980.
[8] P. Perona, J. Malik, Scale-space and edge detection using anisotropic diffusion, Pattern Anal. Mach. Intell. IEEE Trans. 12 (1990) 629–639.
[9] L.M. Schmitt, Theory of genetic algorithms, Theor. Comput. Sci. 259 (2001) 1–61.
[10] G. Stockman, L.G. Shapiro, Computer Vision, first ed., Prentice Hall PTR, Upper Saddle River, NJ, USA, 2001.
[11] P. Viola, M. Jones, Rapid object detection using a boosted cascade of simple features, in: Computer Vision and Pattern Recognition, 2001. CVPR 2001. Proceedings of the 2001 IEEE Computer Society Conference on, 2001 pp. I–511–I–518 vol.1.
[12] M.H. Yang, D. Kriegman, N. Ahuja, Detecting faces in images: a survey, Pattern Anal. Mach. Intell. IEEE Trans. 24 (2002) 34–58.
[13] J. Schenk, in: Dynamika Poklesové Kotliny, Textbook, VŠB - TU Ostrava, HGF, IGDM, 2000, p. 13.
[14] DIAS-DA-COSTA, D., et al. Monitoring of concrete members using photogrammetry and image processing. 2014.
[15] T. Moriyama, et al., Automatic target-identification with the color-coded-targets, in: The International Archives of Photogrammetry and Remote Sensing, Beijing, XXI Congress, WG, 2008, pp. 39–44.